A EUROPEAN JOURNAL OF CHEMICAL BIOLOGY

CHEMBIOCHEM

SYNTHETIC BIOLOGY & BIO-NANOTECHNOLOGY

# Accepted Article

**Title:** A new photocaged puromycin for an efficient labelling of newly translated proteins in living neurons

**Authors:** Harald Schwalbe, Isam Elamri, Maximillian Heumüller, Lisa M Herzig, Elke Stirnal, Josef Wachtveitl, and Erin Schuman



**To be cited as:** *ChemBioChem* 10.1002/cbic.201800408

**Link to VoR:** http://dx.doi.org/10.1002/cbic.201800408

A Journal of

ChemPubSoc Europe

WILEY-VCH

www.chembiochem.org

10.1002/cbic.201800408

WILEY-VCH

COMMUNICATION

# A new photocaged puromycin for an efficient labeling of newly translated proteins in living neurons**

Isam Elamri+,[a] Maximilian Heumüller+,[b] Lisa-M. Herzig,[c] Elke Stirnal,[a] Josef Wachtveitl,[c] Erin M. Schuman,[b] and Harald Schwalbe*,[a]

Monitoring of newly synthesized proteins is becoming increasingly important to characterize proteome composition in regulatory networks. Puromycin is a peptidyl transfer inhibitor, widely used in cell biology for tagging newly synthesized proteins. Here, we report synthesis and application of an optimized puromycin carrying a photolabile protecting group as a powerful tool for tagging nascent proteins with high spatiotemporal resolution. The photocaged 7-N,N-Diethylamino-cumarin-4-yl]-methoxycarbonyl-puromycin (DEACM-puromycin) was synthesized and compared with the previously developed 6-Nitroveratryloxycarbonyl puromycin (NVOC-puromycin). The photo-chemical behaviour as well as the effectiveness in controlling the puromycylation in living hippocampal neurons using two-photon excitation is superior to the previously used NVOC-puromycin. We further report on the application of light-controlled puromycylation to visualize new translated proteins in neurons.

**P**rotein synthesis and degradation are fundamental steps in gene expression.[1] It is thus important to monitor newly synthesized proteins. The aminonucleoside puromycin is a low molecular weight analogue of the 3´-end of tyrosine-loaded tRNA ($tRNA^{tyr}$). Puromycin is nonspecifically incorporated into the growing nascent paptide chain during translation and causes dissociation of the nascent peptide chain from the ribosome. The puromycilated nascent peptide can be detected by anti-puromycin antibodies.[2][3] At low concentration, puromycin is not able to compete with the aminoacyl tRNA but binds specifically at the C-terminus of the full-length protein, stochastically labeling newly synthesized proteins.[4][5][6][7][8] Thus, it provides a snapshot of the translatome. Furthermore, in contrast to isotope amino acid-based labeling methods, puromycin is not RNA codon-dependent. This codon-independence allows an unbiased labeling of newly synthesized proteins. Due to its efficient incorporation, no amino acid starvation needs to be performed prior to labeling.[9]

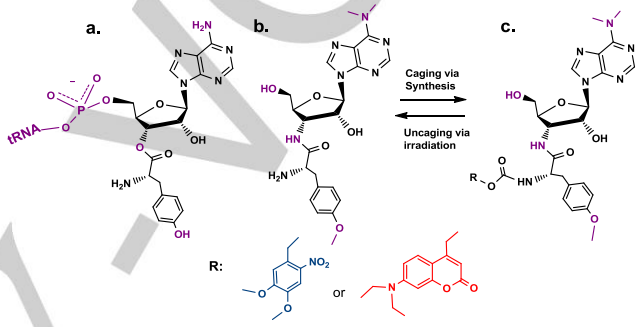


**Scheme 1.** a. Structural similarity between 3´-end of a tyrosyl-tRNA and the aminonucleoside anibiotic puromycin b. Differences are shown in violet. c. Photocaged NVOC- or DEACM-puromycin.

In addition, the commercial availability and the easy handling of puromycin makes puromycylation a powerful method for tagging newly translated proteins. Previously,[10][11] we developed a puromycin protected by a 6-nitroveratryl-oxycarbonyl (NVOC) group (Scheme 1), which is a derivative of the well-known nitrobenzyl (oNb)-photolabile protecting group[12][13][14]. In addition to the spectroscopic investigation of the uncaging mechanism, we showed using two-photon uncaging irradiation-dependent spatiotemporal puromycylation of nascent protein chains in hippocampal neurons. However, the solubility of NVOC-puromycin is modest preventing the use of high concentrations of the caged compound in cell culture experiments. Furthermore, the extinction coefficient (6500 $M^{-1}.cm^{-1}$) and the quantum yield (1.1 ± 0.2%)[11] are low. We demonstrated[10] that the low quantum yield is a result of a triplet photodeactivation pathway allowing efficient relaxation to the ground state after irradiation.

We therefore report here on the development and application of a more suitable photocleavable puromycin. *7-N,N-Diethylamino-4-hydroxymethylcoumarin* (DEACM) is a frequently used photolabile group for application in living organisms. The coumarin-protecting group fulfils most criteria for cellular applications. The high extinction coefficient (2.5 x $10^4$ $M^{-1}cm^{-1}$ at $\lambda_{max}$ = 369 nm)[15] increases the uncaging efficiency, so that a relatively low light dose is sufficient. Furthermore, DEACM can be cleaved off with light at wavelengths higher than 350 nm and exhibits a satisfactory two-photon excitation cross-sections permitting two-photon uncaging.[16][17][18][19]

[a] I. Elamri*, E, Stirnal, Prof. Dr. H. Schwalbe
Center for Biomolecular Magnetic Resonance
Institute of Organic Chemistry and Chemical Biology
Goethe-University Frankfurt am Main (Germany)
Max-von-Laue-Straße 7, 60438 Frankfurt am Main (Germany)
Email: schwalbe@nmr.uni-frankfurt.de
[b] M. Heumüller*, Prof. Dr. E. M. Schuman
Department of Synaptic Plasticity, MPI for Brain Research
Goethe-University Frankfurt am Main (Germany)
Max-von-Laue-Straße 4, 60438 Frankfurt am Mail (Germany)
[c] L.-M. Herzig, Prof. Dr. J. Wachtveitl
Institute of Physical and Theoretical Chemistry
Goethe-University Frankfurt am Main (Germany)
Max-von-Laue-Straße 7, 60438 Frankfurt am Main (Germany)

[+] These authors contributed equally to this work.

We thank Dr. J. Wirmer-Bartoschek for critical reading of the manuscript. This work was supported by DFG in graduate college CLIC and in the collaborative research center SFB902. Work at BMRZ is supported by the state of Hessen.

Supporting information for this article is given via a link at the end of the document.

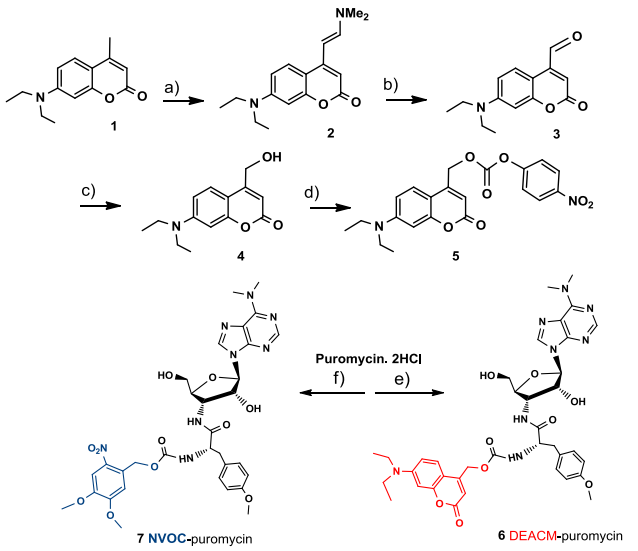


**Scheme 2** Synthesis of 7-N,N-Diethylamino-cumarin-4-yl]-methoxy-carbonyl-puromycin (DEACM-puromycin) and 6-nitroveratyl-oxycarbonyl puromycin (NVOC-puromycin). Reagents and conditions : (a) 7-diethylamino -4 -methylcoumarin (1 equiv.), DMF-DMA (2 equiv.), DMF, 160 °C, 7h; (b) **2** (1 equiv.), $NaIO_4$ (3 equiv.), THF/$H_2O$ 1:1, R.T., 5h; (c) **3** (1 equiv.), $NaBH_4$ (0.5 equiv.), EtOH, RT, 4 h, 98%; (d) **4** ( 1 equiv.), DMAP (2 equiv.), 4-$NO_2$Ph-chloroformate (2 equiv.), $CH_2Cl_2$, RT, 7 h. (e) Puromycin▪2HCl (1 equiv.), DIPEA ( 20 equiv.), 5 (1,2 equiv.), DMAP (2 equiv.), $CH_2Cl_2$, 40 °C, 24 h, 25%. (f) Puromycin.2HCl (1 equiv.), DIPEA (20 equiv.), NVOC-Cl (1, 5 equiv.) $CH_2Cl_2$, RT, 24 h, 75%. Abbreviation: $SeO_2$ = selenium dioxide; $NaBH_4$ = sodium borohydride; $NaIO_4$ = sodium periodate, $NO_2$Ph = Nitrophenyl; DIPEA = N,N-diisopropylethylamine; DMF-DMA = N,N-dimethylformamide dimethyl acetal; DMAP = N,N-dimethylamino-pyridine. Characterization of the data is presented in the Supporting Information (Figures S4-11).

We synthesized DEACM-puromycin in five steps. Starting from 7-Amino-4-methylcoumarin, the allylic methyl group can be oxidized via the Riley-reaction using selenium dioxide to generate the aldehyde **3** with a yield of 29%. An alternative route avoiding the use of toxic selenium dioxide and featuring a higher yield, is the two step procedure reported by *Weinrich et al.*,[20] starting with the condensation to enamine **2** using DMF-DMA followed by treatment with the oxidizing agent sodium periodate. In both cases, the obtained aldehyde **3** is reduced via sodium borohydride to give the alcohol **4** in 98%. Since amines are most effectively photolabile-protected via a carbamate linker, it is necessary to first modify the alcohol **4** to DEACM-4´-nitrophenyl carbonate **5**, which then reacts without further purification with puromycin▪HCl in the presence of DIPEA and DMAP to yield the final product **6** with a total yield of 25%. NVOC-puromycin was synthesized according to the published procedure [7] using NVOC-Cl in the presence of DIPEA (75%, yield). Uncaging of both caged puromycin types was verified by using reversed HPLC and a laser-coupled NMR setup. (See the Supporting Information Figures S12-15). As shown in Figure 1, the absorption of NVOC- and DEACM-puromycin share similar spectral features beyond 300 nm, which results from the puromycin moiety in both compounds. However, the absorption maximum at 375 nm of DEACM-puromycin is 30 nm red-shifted compared to NVOC-puromycin. Moreover, the coumarin caged-compound shows strong absorption characteristics above 400 nm. Therefore, the uncaging of DEACM-puromycin can be induced with visible light, which is in particular favorable for biological applications. Hence, application of DEACM-puromycin prevents photodamage of the tissue. In addition, the extinction coefficient of DEACM-puromycin is more than three times larger than the extinction coefficient of NVOC-puromycin.[11][21] Accordingly, uncaging of the coumarin caged-compound can be induced by a less harmful light dose as compared to NVOC-puromycin. To quantify the uncaging

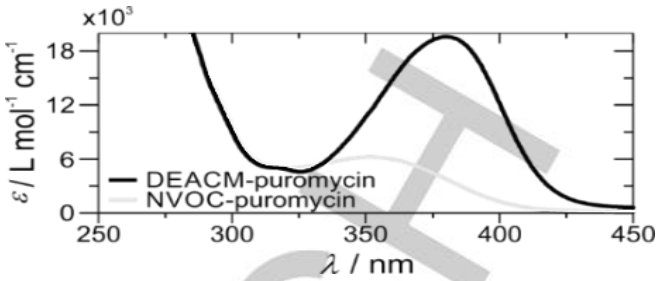


**Figure 1**. Absorption spectra of NVOC-puromycin (gray) and DEACM-puromycin (black) in DMSO, where ε is the molar extinction coefficient and λ the wavelength.

efficiency, the uncaging quantum yield has been determined. Because the absorption of the photoproduct DEACM-OH is indistinguishable of DEACM-puromycin, the quantum yield cannot be measured in the UV/vis-range. Therefore, both compounds have been irradiated with 365 nm and the absorption changes in the IR-range have been recorded (Figure S1). Besides other spectral changes, the decarboxylation process of the carbamate linker in both molecules can be monitored at 2337 $cm^{-1}$, which is the characteristic absorption of dissolved $CO_2$.[22]

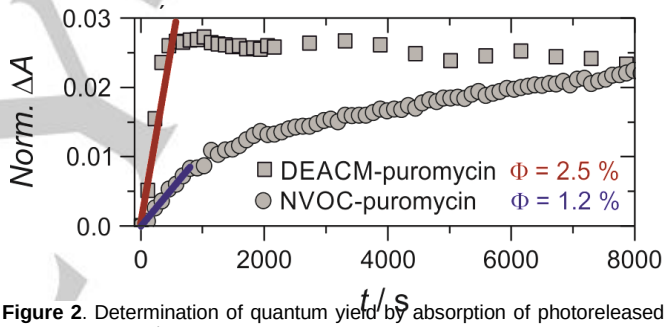


**Figure 2**. Determination of quantum yield by absorption of photoreleased $CO_2$ at 2337 $cm^{-1}$ during UV excitation of NVOC-puromycin (circles) and DEACM-puromycin (squares) with corresponding fits. The concentrations of the compounds have been considered for scaling. In the supporting information detailed information for the determination of the quantum yield and the IR absorption spectra evolving during excitation of cage puromycin are given.

As shown in Figure 2, the increase of the carbon dioxide absorbance observed in the first 10 min of irradiation, can be described with a linear function. On this timescale the assumption that the caged compounds are the dominant absorbing species is valid, because the photolysis has not yet led to a significant product formation. Consequently, the absorbance change at 2337 $cm^{-1}$ is only caused by product formation and therefore, is directly related to the number of uncaging photoreactions taking place. We determined an uncaging quantum yield of 2.5 ± 0.4% for DEACM-puromycin and 1.2 ± 0.1% for NVOC-puromycin (for calculation see Supporting Information Eq. 1-4). The uncaging efficiency as the product of extinction coefficient and quantum

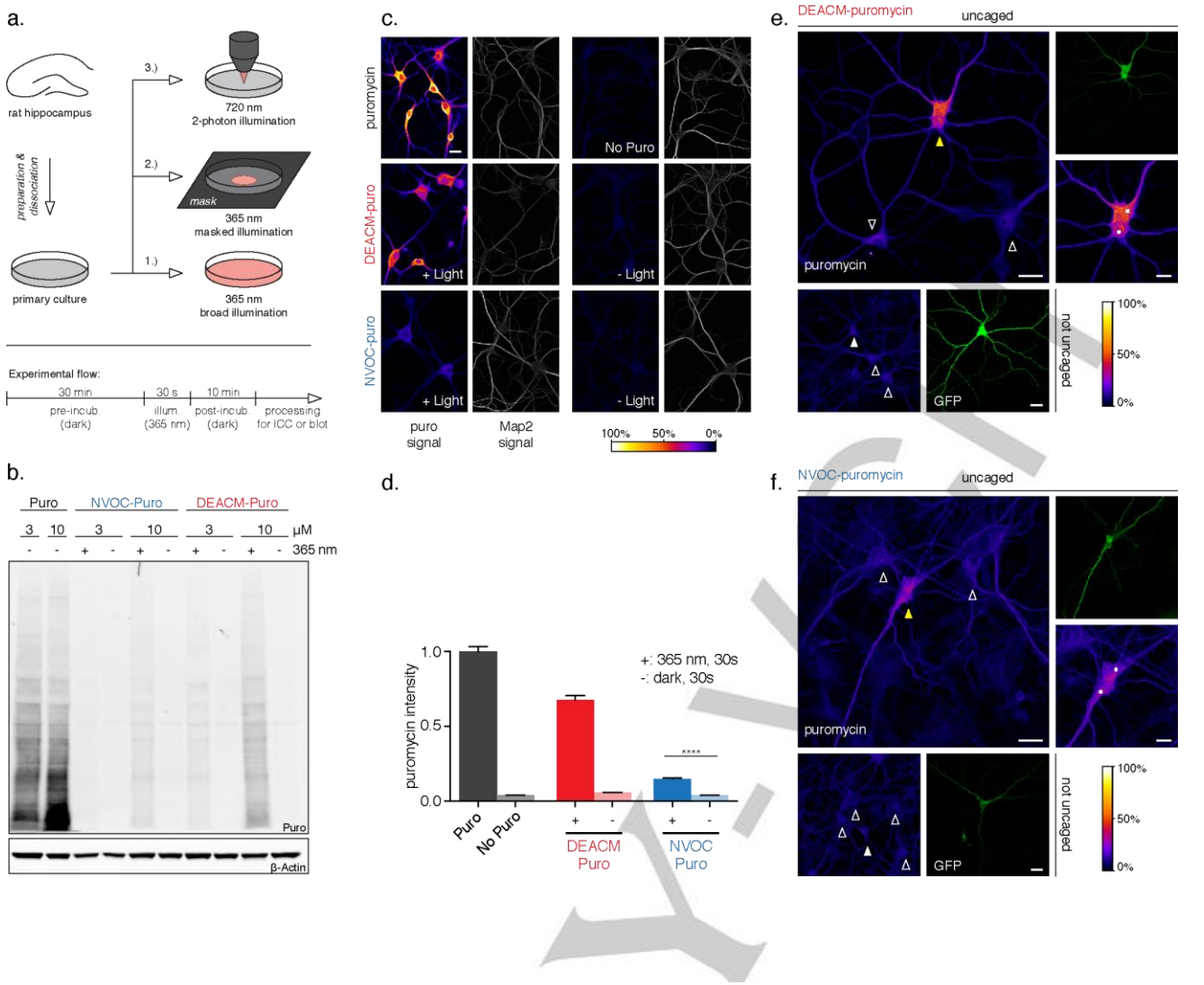


**Figure 3.** a. Scheme of the experimental workflow. Primary cultured neurons are prepared from hippocampal brain tissue and used for three types of experiments. Broad illumination at 365nm (1.) or partial illumination at 365nm using a mask (2.) For high spatial resolution two-photon uncaging at 720nm (3.) was applied. A general time line for experiments is depicted at the bottom of b. Western blot showing the puromycin signal of 20ug of protein as well as the ß-Actin signal as a loading control. c. Maximum intensity projections of immunocytochemically (ICC) stained primary hippocampal neurons. Puromycylated protein is labeled (anti-puromycin antibody) and the intensity is depicted with a fire look-up table (LUT) (calibration bar indicates signal intensity in %), Anti-Map2 labeling, highlighting neuronal dendrites,is shown gray. The specific conditions are indicated with the images: 'No Puro' means no puromycin has been added to the medium, '+Light' neurons were illuminated 30s at 365nm, '-Light' cultures were treated the same way but were not illuminated. Scale bar represents 10um. d. Statistic analysis (Mann-Whitney U test for NVOC-Puro) of (c.) with each column representing data from 52-62 neurons and showing the average puromycin signal normalized to the puromycin intensity of the (uncaged) puromycin treated cells. The error bars indicted SEM and significance was determined using a Mann-Whitney U test. e. Maximum intensity projections of immunocytochemically labeled primary hippocampal neurons that were pre-incubated with 3µM DEACM-puromycin. Puromycin signal is highlighted by a fire-LUT (anti-puromycin antibody) and GFP-transfected cells are visualized in green (GFP fluorescence), GFP transfected cells are marked in the puromycin channel by filled triangles and un-transfected cells by empty triangles. Uncaging in transfected neurons was conducted (yellow, filled triangle) by 720nm two-photon illumination on two 1um$^2$ spots within the cell body. In control cells no illumination was (white, filled triangle). Scale bare is 20um. f. Same as (e.) but NVOC-puromycin instead of DEACM-puromycin.

yield is for DEACM-puromycin more than six times larger than for NVOC-puromycin. This is, in theory, beneficial for the use in cellular application. Following the direct comparison of both caging compounds using analytic chemistry, we set out to evaluate their performance in a cellular environment. Protein synthesis plays, for example, a crucial role in learning and memory formation, thus there is a great demand for tools to monitor translation with high temporal and spatial resolution in neuroscience.[23][24] We used primary rat cultured hippocampal neurons to investigate the uncaging properties. First, we demonstrate that DEACM-puromycin is taken up by the cell as previously shown for NVOC-puromycin (Figure S2). The illumination dependence of both puromycin-derivaties was compared by broad illumination of the whole culture dish, partial

illumination using a physical mask, or precise single cell illumination using two-photon uncaging (Figure 3a.). Immunocytochemical staining with an anti-puromycin antibody, revealed that native puromycin exhibits the strongest labeling, followed by irradiated DEACM-puromycin which is more than 3 times more efficient than irradiated NVOC- puromycin (Figure 3. c, d.). This observed difference in labeling correlates well with the observed difference in uncaging efficiency of the compounds. Similar results were obtained using Western blotting (Figure 3. b.), with DEACM-caged puromycin showing significantly stronger signal than its predecessor for both concentrations (3μM/10μM). Cellular uptake of caged-puromycin enables precise spatial puromycylation, which we demonstrated by placing a physical mask between the light source and the dish allowing only illumination of a small region. Using this partial masking we were able to confine puromycilation to the illuminated area of the dish (Figure S3) exhibiting the same spatial potential as its predecessor. To evaluate any potential impact of the illumination procedure on the cell health of our neuronal cultures, we performed an apoptosis assay. As expected, this revealed that our robust UV irradiation protocol did not induce cell death and had no impact on DNA integrity (Figure S16). Furthermore, the uptake efficiency for both cages was quantified by measuring the remaining amount of puromycin in the supernatant after 1h of incubation on culture dishes with neurons or empty dishes as a control. The cells take up around 55% of the native Puromycin present in the medium during 1h of incubation, while only 45% of NVOC-puromycin and 30% of DEACM-puromycin are taken up during the same time period (Figure S17). This indicates that the improved uncaging efficiency of DEACM-puromycin is mainly responsible for the enhanced labeling in cell culture, since DEACM-cage uptake is slightly reduced compared to the NVOC-cage but nonetheless yields a stronger labeling.

In order to demonstrate the subcellular spatial resolution of uncaging, two-photon illumination at 720 nm was performed (Figure 3. e, f.). GFP-transfected neurons were selected and uncaging of both caged puromycin-derivatives revealed elevated puromycin levels specifically within the targeted cells (yellow triangle), in close proximity to the uncaging spots. Neurons that were GFP transfected but not targeted (white triangle) showed no increased puromycilation similar to cells that were neither transfected nor targeted (empty triangle). Again, using the same wavelength and intensity, DEACM-puromycin exhibited a significantly stronger labeling and a comparable low background signal in non-illuminated regions. If less strong labeling is preferred the light intensity, duration or illumination region can be adjusted to achieve the desired result.

In conclusion, we have developed and synthesized an improved caged puromycin (DEACM-cage) that offers superior labeling properties due to its higher cleavage efficiency of the cage with no drawbacks compared to its predecessor (NVOC-cage). This suggests that DEACM-puromycin likely the best molecule of choice, since less harmful light doses can be used for the same amount of uncaging. DEACM-caged puromycin also exhibits a red-shifted excitation maximum compared to NVOC-caged puromycin allowing the use of single-photon uncaging within the visible range. This again exposes the cell to less stress during the uncaging process compared to the ultraviolet illumination needed for the NVOC-cage. The increased sensitivity also opens up new possibilities for the use in fragile areas of the cell or compartments with low protein synthesis-rates, e.g. distal dendrites. Experiments that require very brief labeling periods also benefit from the elevated uncaging efficiency. The advantages conferred by this new cage make existing experiments more amenable and may allow for novel experimental designs including investigation of local protein synthesis at the base of spines or in the distal parts of the dendritic branch, which is believed to be a key mechanism involved in the formation and maintenance of memories.[25][26]

## Experimental Section

**Synthesis of DEACM-puromycin (6)**

**Method A: 7-N,N-Diethylamino-cumarin-4-yl]-methoxycarbonyl-puromycin (DEACM-puromycin) (2):** To a solution of 7-Amino-4-methyl-coumarin (20.00 g, 86.48mmol, 1 equiv.) in dry DMF (150 mL), DMF-DMA (23 mL, 0.173 mol, 2 equiv.) was added. The mixture was heated to reflux for 48 h. The reaction was then quenched with the addition of conc. $NaHCO_3$ solution and extracted twice with 1 L of $CH_2Cl_2$. The combined organic layers were dried over $NaSO_4$ and evaporated to yield a brown solid. The product was then isolated by recrystallization from EtOAc/*c*-hex 1:2 (19.2 g, 78%). Rf = 0.38 ($CH_2Cl_2$/EtOAc, 7:3). $^1$H NMR (500 MHz, $CDCl_3$): δ = 7.53 (d, J = 9.1 Hz, 1 H, 5-**H**), 7.21 (d, J = 13.0 Hz, 1 H, CHC**H**N), 6.55 (dd, J = 9.0, 2.7 Hz, 1 H, 6-**H**), 6.49 (d, J = 2.7 Hz, 1 H, **H**-8), 5.85 (s, 1 H, 3-H), 5.22 (d, J = 13.0 Hz, CHC**H**N), 3.40 (q, J = 7.1 Hz, 4 H, C**H**$_2$CH$_3$), 2.98 (s, 6 H, N(C**H**$_3$)$_2$), 1.20 (t, J = 7.0 Hz, 6 H, CH$_2$C**H**$_3$) ppm. $^{13}$C NMR (125.8 MHz, $CDCl_3$): δ = 163.4, 156.4, 152.2, 150.1, 146.7, 124.7, 108.1, 107.8, 98.0, 93.5, 87.7, 44.6, 12.5 ppm. MS (ESI): *m/z* = calcd. for $C_{17}H_{23}N_2O_2$ [$M^+$ $H^+$]: 287.18; found 287.24.

**7-(diethylamino)-2-oxo-*2H*-chromene-4-carbaldehyde (3)*:** $NaIO_4$ (5.60 g, 26.20 mmol, 3 equiv.) was added to a suspension of enamine **2** (5.00 g, 17.50 mmol, 1 equiv.) in a mixture of THF and $H_2O$ (40 mL, 1:1). A cloudy red precipitate immediately formed. The reaction was stirred at room temperature for 1 h. The precipitate was removed by filtration and extracted twice with EtOAc. Subsequently, conc. $NaHCO_3$ solution was added and the aqueous layer was extracted twice with EtOAc. The combined organic layers were dried over $MgSO_4$ and concentrated in vacuo. The crude product was purified by silica gel chromatography (EtOAc/*c*-hexane, 1:1), which yielded the title compound **3** (6.05 g, 75%). The product was obtained as a red oil. Rf = 0.40 ($CH_2Cl_2$, 100%). $^1$H NMR (600 MHz, $CDCl_3$): δ = 10.1 (s, 1 H, CO**H**), 8.22 (d, J = 9.2 Hz, 5-**H**), 6.78 (dd, J = 9.2, 2.6 Hz, 1 H, 6-**H**), 6.65 (s, 1 H, 3-**H**), 6.61 (d, J = 2.6 Hz, 1 H, 8-**H**), 3.46 (q, J = 7.1 Hz, 4 H, C**H**$_2$CH$_3$), 1.15 (t, J = 7.1 Hz, 6 H, CH$_2$C**H**$_3$) ppm. $^{13}$C NMR (125.8 MHz, $CDCl_3$): δ = 192.5, 161.8, 157.4, 151.0, 143.9, 126.2, 117.3, 109.5, 103.7, 98.2, 44.8, 12.4 ppm. MS (ESI): *m/z* = calcd. for $C_{14}H_{16}NO_3$ [$M^+$ $H^+$]: 246.11; found 246.16.

*****Compound **(3)** was also synthesized based on the procedure reported by *Weinrich et al*.,[20] where no purification by silica gel chromatography needs to be performed.

**7-(diethylamino)-4-(hydroxymethyl)-*2H*-chromen-2-one (4):** A solution of aldehyde **3** (1.12 g, 4.60 mmol, 1 equiv.) was dissolved in THF (15 mL) and cooled to 0 °C. $NaBH_4$ (0.35 g, 9.19 mmol, 2 equiv.) was added and the reaction mixture

was stirred under argon for 2 h at room temperature, quenched with saturated $NaHCO_3$ and the organic layer was separated. The aqueous layer was extracted with $CH_2Cl_2$ and the organic phase was dried over $Na_2SO_4$ and concentrated in vacuo. The crude product was purified by silica gel chromatography ($CH_2Cl_2$/acetone, 5:1), which yielded the compound **4** (1.12 g, quant.). Product was obtained as a yellow solid.

**Method B: Riley oxidation with $Se_2O$ and reduction with $NaBH_4$:** 7-Amino-4-methyl-coumarin (4.63 g, 20.0 mmol, 1 equiv.) and selenium dioxide (3.33 g, 30.0 mmol, 1.5 equiv.) were dissolved in *p*-xylene (120 mL). The reaction mixture was heated to reflux with vigorous stirring for 24 h. The precipitate was filtered off and concentrated under reduced pressure. The obtained dark brown oil and $NaBH_4$ (380 mg, 10.0 mmol, 0.5 equiv.) were dissolved in ethanol (130 mL) and stirred for 4 h at ambient temperature. Subsequently 1 M HCl (20 mL) was added to the suspension, and diluted with $H_2O$ and extracted three times with $CH_2Cl_2$. The organic layers were washed with $H_2O$ and brine, dried over $Na_2SO_4$ and reduced to an oil by rotary evaporation. The crude product was purified by silica gel chromatography ($CH_2Cl_2$/acetone, 5:1) (1.28 g, 26%). Rf = 0.28 (*c*-hexane/EtOAc, 1:2). $^1$H NMR (600 MHz, DMSO-$d_6$): 7.48 (d, J = 9.0 Hz, 1 H, 5-**H**), 6.70 (dd, J = 9.0, 2.6 Hz, 1 H, 6-**H**), 6.56 (d, J = 2.6 Hz, 1 H, 8-**H**), 6.12 (s, 1 H, 3-H), 5.55 (t, J = 5.6 Hz, 1H, O**H**), 4.73 (dd, J = 5.6, 1.3 Hz, 2 H, C**H**$_2$OH), 3.46 (q, J = 7.1 Hz, 4 H, C**H**$_2$CH$_3$), 1.17 (t, J = 7.1 Hz, 6 H, CH$_2$C**H**$_3$) ppm. $^{13}$C NMR (125.8 MHz, DMSO-$d_6$): δ = 161.1, 156.8, 155.6, 150.2, 125.0, 108.5, 105.7, 103.9, 96.8, 59.0, 43.9, 12.3 ppm. MS (ESI): *m/z* = calcd. for $C_{14}H_{18}NO_3$ [$M^+$ $H^+$]: 248.13; found 248.19.

**7-(diethylamino)-4-[(ylmethyl-(4´-nitrophenyl)]-*2H*-chromen-4-ylcarbonate (5):** A mixture of alcohol **4** (22.7 mg, 0.09 mmol, 1 equiv.), DMAP (22.5 mg, 0.18 mmol, 2 equiv.) and 4-nitrophenyl chloroformate (22.3 mg, 0.11 mmol, 1.2 equiv.) in dry $CH_2Cl_2$ (3 mL) were stirred under argon atmosphere and in the absence of light overnight at room temperature. After 20 h silica gel TLC (*c*-hexane/EtOAc, 1:1 (Rf = 0.80)) showed the reaction to be complete. To remove the chloride salt of dimethylaminopyridinium, the mixture was washed twice with $H_2O$ (2 x 100 mL). The organic layers were evaporated to a brown solid. NMR-based estimated yield of compound **5** was ca. 60%. The crude product was used in the next step without further purification. An analytical sample was purified by silica gel chromatography ($CH_2Cl_2$/MeOH, 49:1). Rf = 0.80 (*c*-hexane/EtOAc, 1:1). $^1$H NMR (600 MHz, $CDCl_3$): δ = 8.23 (d, J = 9.15 Hz, 2 H, Ar**H** *o* to –$NO_2$), 7.35 (d, J = 9.15 Hz, 2 H, Ar**H** *m* to –$NO_2$), 7.26 (d, J = 9.0 Hz, 1 H, 5-**H**), 6.59 (dd, J = 9.0, 2.4 Hz, 1 H, 6-**H**), 6.50 (d, J = 2.4 Hz, 1 H, 8-H), 6.17 (s, 1 H, 3-H), 5.33 (d, J = 1.1 Hz, 2 H, C**H**$_2$OH), 3.36 (q, J = 7.2 Hz, 4 H, C**H**$_2$CH$_3$), 1.15 (t, J = 7.1 Hz, 6 H, CH$_2$C**H**$_3$) ppm. MS (ESI): *m/z* = calcd. for $C_{21}H_{20}N_2O_7$ [$M^+$ $H^+$]: 413.08; found 413.06.

**7-N,N-Diethylamino-cumarin-4-yl]-methoxycarbonyl-puromycin (DEACM-puromycin) (6):** To a suspension of puromycin·2HCl (25mg, 0.046 mmol, 1 equiv.) in dry $CH_2Cl_2$ (1 mL), DIPEA (175 µL, 0.92 mmol, 20 equiv.) was added under stirring to give a clear solution and kept under $N_2$-atmosphere. A solution of scrude product **5** (ca. 23 mg, 0.054 mmol, 1.2 equiv.) and DMAP (13.2 mg, 0.11 mmol, 2.4 equiv.) was prepared and added dropwise to the puromycin solution to avoid an additionally 5´-*O*-acylation. The reaction mixture was stirred at room temperature under $N_2$-atmosphere for 20 h. Light exposure was minimized. The brown solution was diluted with $CH_2Cl_2$ (25 mL) and washed with conc. $NaHCO_3$ solution, brine and $H_2O$ (2 x 50 mL). The organic layers were dried over $MgSO_4$ and concentrated in vacuo. The crude product was obtained as yellow oil. Silica gel chromatography ($CH_2Cl_2$/MeOH, 9:1), subsequently reversed-phase HPLC ($H_2O$/ACN) and lyophilization afforded the title compound **6** as white needles (8.50 mg, 25%). Rf = 0.70 ($CH_2Cl_2$/MeOH, 9:1), rp-HPLC: [Kromasil RP18, 4.60 x 250 mm, gradient: ($H_2O$/ACN, 30-100%), ACN in 50 min, 3 mL/min, Rt = 29.90 min], $^1$H NMR (500 MHz, DMSO-$d_6$): δ = 8.48 (s, 1 H, **H**-8), 8.27 (s, 1 H, **H**-2), 8.26 (br, 1 H, 3´-N**H**CO),7.80 (d, J = 8.83 Hz, 1 H, N**H**COO), 7.41 (d, J = 9.04 Hz, 1 H, Coum**H**-5), 7.27 (d, J = 8.6 Hz, 2 H, *m*-(ph(OMe)-2**H**))), 6.87 (d, J = 8.6 Hz, 2 H, *o*-(ph(OMe)-2**H**))), 6.69 (dd, J = 9.04, 2.5 Hz, 1 H, Coum**H**-6), 6.56 (d, J = 2.5 Hz, 1 H, Coum**H**-8), 6.15 (br, 1 H, 2´-OH), 6.03 (d, J = 2.67, 1 H, 1´**H**), 5.98 (s, 1 H, Coum**H**-3), 5.24 (t, J = 5.30, 1 H, 5`-OH), 5.17 (d, J = 6.67, 2 H, CoumC**H**$_2$), 4.5 (br, 2 H, 2- H´, 3-H´), 4.38 (td, J = 9.62, 4.10 Hz, 1 H, OMeTyr-**H**(α)), 3.99 (m, 1 H, 4´-H), 3.74 (s, 3 H, O**Me**), 3.70 (m, 1 H, 5´**H**2-OH), 3.51 (m, 1 H, 5´**H**2-OH), 3.45 (q, J = 7.2 Hz, 4 H, C**H**$_2$CH$_3$), 3.33 (s, 6 H, (NC**H**$_3$)$^{2+}$ water) 2.98 (dd, J = 13.66, 4.1 Hz, 1 H, OMeTyr-H(β)), 2.75 (m, 1 H, OMeTyr-H(β)), 1.14 (t, J = 7.1 Hz, 6 H, CH$_2$CH$_3$) ppm. $^1$H NMR resonances were assigned using $^1$H-$^{13}$C-HSQC, COSY, HMBC spectra recorded at 500 MHz in DMSO-$d_6$. MS (ESI): *m/z* = calcd. for $C_{37}H_{44}N_8O_9$ [$M^+$ $H^+$]: 745.22; found 745.20.

**Synthesis of NVOC-puromycin (7) 4,5-dimethoxy-2-nitrobenzyl-oxycarbonyl-puromycin.** To a suspension of Puromycin. 2HCl (50mg, 0.092 mmol, 1 equiv.) in 2 mL dried Dichlormethan, DIPEA (160uL, 0.92 mmol, 10 equiv.) was added and stirred 5 min under $N_2$-atmosphere to give a clear solution. To this was added NVOC-Cl (37.8 mg, 0.13 mmol, 1.5 equiv.) and the yellow mixture was stirred overnight under $N_2$-atmosphere at room temperature. Light exposure was minimized. The brown solution was diluted with $CH_2Cl_2$ (25 mL) and washed with conc. $NaHCO_3$ solution, brine and $H_2O$ (2 x 50 mL). The organic layers were dried over $MgSO_4$ and concentrated in vacuo. The crude product was obtained as yellow oil. Silica gel chromatography ($CH_2Cl_2$/MeOH, 9:1), subsequently reversed-phase HPLC ($H_2O$/ACN) and lyophilization afforded the title compound 6 as white needles (49 mg, 75%). Rf = 0.66 (n-Hex/EE: 1/3), rp-HPLC: [Kromasil RP18, 10 x 250 mm, gradient: ($H_2O$/ACN, 30-100%), ACN in 50 min, 3 mL/min, Rt = 20.5 min], $^1$H NMR (500 MHz, DMSO-$d_6$): δ = 8.44 (s, 1 H, H-8), 8.26 (br, 1 H, 3´-NHCO), 8.25 (s, 1 H, H-2), 7.78 (d, J = 8.76 Hz, 1 H, NHCOO), 7.69 (s, 1 H, $NO_2$Ar-H), 7.24 (d, J = 8.3 Hz, 2 H, *m*-(ph(OMe)-2H))), 7.13 (s, 1 H, $NO_2$Ar-H), 6.81 (d, J = 8.4 Hz, 2 H, *o*-(ph(OMe)-2H))), 6.10 (d, J = 4.5 Hz, 1 H, 1´H), 6.00 (d, J = 2.3 Hz, 1 H, 2´-OH), 5.28 (s, , 2 H, NVOC-CH$_2$), 5.18 (t, J = 5.4 Hz, 1 H, 5`-OH), 4.9 (m, 2 H, 2- H´), 4.36 (td, J = 9.62, 4.10 Hz, 1 H, OMeTyr-H(α)), 3.94 (m, 1 H, 4´-H), 3.86 (s, 6 H, (OCH$_3$)2), 3.70 (s, 3 H, OMe), 3.68 (m, 1 H, 5´H2-OH), 3.47 (m, 1 H, 5´H2-OH), 3, 30 (6H, (NCH$_3$)2+water), 2.94 (dd, $^3$J = 13.8 Hz, $^4$J = 4.1 Hz, 1 H, OMeTyr-H (β)), 2.72 (m, 1 H, OMeTyr-H(β)),

ppm. $^{1}$H NMR resonances were assigned using $^{1}$H-$^{13}$C-HSQC, COSY, HMBC spectra recorded at 500 MHz in DMSO-$d_6$. $^{13}$C NMR (125.8 MHz, DMSO-$d_6$): δ = 50.8, 55.4, 56.5, 56.8, 61.4, 62.8, 73.5, 83.9, 88.9, 108.6, 110.5, 113.9, 120.1, 128.7, 130.3, 130.8, 138.4, 139.4, 148.1, 150.2, 152.5, 154.0, 154.8, 155.9, 158.3, 172.4 ppm. MS (ESI): *m/z* = calcd. for $C_{32}H_{38}N_8O_{11}$ [$M^+$ $H^+$]: 711.69; found 711.15.

Characterization data for all synthesized compounds can be found in the Supporting Information.

**UV/vis spectroscopy.** UV/vis spectra were recorded with a Specord S600 spectrophotometer (Analytik Jena).

**FTIR measurements.** IR spectra were recorded with a Vertex 80 FTIR spectrometer (Bruker, Ettlingen). The spectrometer was continuously purged with $N_2$. Photolysis experiments were carried out using a 365 nm LED (Thorlabs GmbH).

**Cell Culture & transfection.** Primary cultures were prepared from rat hippocampus tissue and seeded at 40k cells on a 12mm glas coverslip (Mattek dish) for imaging experiments or 600k for western blot analysis. The cells were cultured at 37C and 5% $CO_2$ in Neuro Basal A medium for 11 days (DIV11). At DIV 11 the cells (1 dish contains 40k cells) were transfected with 1ug of the calcium indicator GFP for 25 min using a combination of Magnetofecatim (OZ Bioscience) and Lipofectamin 2000 (Thermo Fisher). Subsequently the medium was replaced and cells were allowed to express the GFP for 12h.

**In vitro experimental flow.** Primary hippocampal cultures were pre-incubated in the dark for 30 or 60min with 3 or 10uM of either NVOC- or DEACM-caged puromycin, followed by 30s of broad whole dish illumination with 365 nm and a 10 min post-illumination incubation to allow for incorporation of the uncaged puromycin. A control dish was incubated with 3uM native puromycin for 10 min. For ICC cells were briefly washed with pre-warmed PBS (pH 7.4), fixed for 20 min with 4% PFA in PBS (pH 7.4) and permeabilized for 15 min with 0.5% Triton X-100 in blocking buffer (4% goat serum in PBS pH 7.4). Primary antibodies used for Map2 (188004, SYSY)) were used 1:1000 and for Puromycin (EQ0001, Kerafast) 1:2000 for 12h in blocking buffer at 4C. Common secondary Alexa-antibodies were used at 1:1000 for detection (45 min at RT). For westernblot cells were treated the same, but instead of fixation they were harvested in lysis buffer (1% SDS, 1% Triton X-100 in PBS pH7.4). The same puromycin antibody was used and bActin-antibody (Ab8227, Abcam) was used at 1:5000 for 12h at 4C. Primary antibodies were detected using Licor IRDye antibodies (IRDye 800 & IRDye680) at 1:5000.

**Imaging & uncaging.**Broad illumination (full dish) was achieved by placing the cell culture dish (with or without light impermeable mask) on a UV-light table and illuminating the dish for 30s with 365nm. Precise subcellular illumination was achieved using a Spinning disk system from Zeiss/3i in combination with a 2p laser from Coherent. Uncaging was performed on two 1um$^2$ sized spots with 10 pulses (10ms) at a 60s interval. Fixed and stained cells were imaged a confocal laser scanning microscope from Zeiss (LSM 780).

**Apoptosis Assay (TUNEL).** Primary hippocampal cultures and broad UV uncaging were performed as described above. The "Click-iT™ TUNEL Alexa Fluor™ 647 Imaging Assay" from Thermo Scientific (C10247) was used according to the manual to detect DNA-strand breaks and evaluate cell health. An antibody co-staining with Map2 (188004, SYSY, 1:1000) was performed.

[1] R. Aviner, T. Geiger, O. Elroy-Stein, *Nat. Protoc.* **2014**, *9*, 751–760.
[2] W. Traub, *Nature* **1963**, *198*, 1165–1166.
[3] D. Nathans, *Pnas* **1964**, *51*, 585–592.
[4] E. Miyamoto-Sato, N. Nemoto, K. Kobayashi, H. Yanagawa, *Nucleic Acids Res.* **2000**, *28*, 1176–1182.
[5] W. J. Hansen, V. R. Lingappa, W. J. Welch, *J. Biol. Chem.* **1994**, *269*, 26610–26613.
[6] N. Nemoto, E. Miyamoto-Sato, H. Yanagawa, *FEBS Lett.* **1999**, *462*, 43–46.
[7] E. K. Schmidt, G. Clavarino, M. Ceppi, P. Pierre, *Nat. Methods* **2009**, *6*, 275–277.
[8] S. Tom Dieck, L. Kochen, C. Hanus, M. Heumüller, I. Bartnik, B. Nassim-Assir, K. Merk, T. Mosler, S. Garg, S. Bunse, et al., *Nat. Methods* **2015**, *12*, 411–414.
[9] J. Ge, C. W. Zhang, X. W. Ng, B. Peng, S. Pan, S. Du, D. Wang, L. Li, K. L. Lim, T. Wohland, et al., *Angew. Chemie - Int. Ed.* **2016**, *55*, 4933–4937.
[10] J. Kohl-Landgraf, F. Buhr, D. Lefrancois, J.-M. Mewes, H. Schwalbe, A. Dreuw, J. Wachtveitl, *J. Am. Chem. Soc.* **2014**, *136*, 3430–3438.
[11] F. Buhr, J. Kohl-Landgraf, S. Tomdieck, C. Hanus, D. Chatterjee, A. Hegelein, E. M. Schuman, J. Wachtveitl, H. Schwalbe, *Angew. Chemie - Int. Ed.* **2015**, *54*, 3717–3721.
[12] A. Patchornik, B. Amit, R. B. Woodward, *J. Am. Chem. Soc.* **1970**, *92*, 6333–6335.
[13] J. F. Cameron, J. M. J. Fréchet, *J. Am. Chem. Soc.* **1991**, *113*, 4303–4313.
[14] C. G. Bochet, *J. Chem. Soc. Perkin Trans. 1* **2002**, 125–142.
[15] N. Gagey, P. Neveu, L. Jullien, *Angew. Chemie - Int. Ed.* **2007**, *46*, 2467–2469.
[16] B. G. Ralph O. Schönleber, Jürgen Bendig, Volker Hagen, *Bioorganic Med. Chem.* **2002**, *10*, 97–101.
[17] C. Brieke, F. Rohrbach, A. Gottschalk, G. Mayer, A. Heckel, *Angew. Chemie* **2012**, *124*, 8572–8604.
[18] S. Weis, Z. Shafiq, R. a. Gropeanu, A. del Campo, *J. Photochem. Photobiol. A Chem.* **2012**, *241*, 52–57.
[19] C. A. Hammer, K. Falahati, A. Jakob, R. Klimek, I. Burghardt, A. Heckel, J. Wachtveitl, *J. Phys. Chem. Lett.* **2018**, *9*, 1448–1453.
[20] T. Weinrich, M. Gränz, C. Grünewald, T. F. Prisner, M. W. Göbel, *European J. Org. Chem.* **2017**, *2017*, 491–496.
[21] L.-M. Herzig, I. Elamri, H. Schwalbe, J. Wachtveitl, *Phys. Chem. Chem. Phys.* **2017**, *19*, 14835–14844.
[22] M. Falk, A. G. Miller, *Vib. Spectrosc.* **1992**, *4*, 105–108.
[23] M. A. Sutton, E. M. Schuman, *Cell* **2006**, *127*, 49–58.
[24] B. W. Agranoff, *Sci. Am.* **1967**, *216*, 115–122.
[25] G. Aakalu, W. B. Smith, N. Nguyen, C. Jiang, E. M. Schuman, *Neuron* **2001**, *30*, 489–502.
[26] C. E. Holt, E. M. Schuman, *Neuron* **2013**, *80*, 648–657.